Int J Thermophys (2009) 30:949–968
DOI 10.1007/s10765-009-0596-0

Thermal Conductivity of Standard Sands. Part I. Dry-State Conditions

Vlodek R. Tarnawski · T. Momose · W. H. Leong · G. Bovesecchi · P. Coppa

Received: 3 November 2008 / Accepted: 13 May 2009 / Published online: 25 June 2009

Abstract A comprehensive thermal conductivity (λ) database of three dry standard sands (Ottawa *C-109*, Ottawa *C-190*, and *Toyoura*) was developed using a transient line heat source technique. The database contains λ data representing a variety of soil compactions and temperatures (T) ranging from 25 °C to 70 °C. The tested standard sands, due to their repeatable physical characteristics, can be used as reference materials for validation of thermal probes applied to similar dry granular materials. The measured data show an increasing trend of thermal conductivity at dryness (λ_{dry}) against T in spite of declining quartz λ with T. The air content (porosity) controls the λ of dry sands by acting as a very effective thermal insulator around solid soil particles. As a result, a diminutive increase of λ_{dry} with T is driven by increasing λ of air. The experimental λ data of dry sands were exceptionally well predicted by de Vries and Woodside–Messmer models, and also by a thermal conductance model, a product of λ of solids and the thermal conductance factor.

Keywords Quartz sands · Series parallel model · Thermal conductivity · Transient line heat source technique

V. R. Tarnawski (✉) · T. Momose
Division of Engineering, Saint Mary's University, 923 Robie Street, Halifax B3H 3C3, Canada
e-mail: vlodek.tarnawski@smu.ca

W. H. Leong
Department of Mechanical and Industrial Engineering, Ryerson University, 350 Victoria Street, Toronto M5B 2K3, Canada

G. Bovesecchi · P. Coppa
Department of Mechanical Engineering, University of Rome "Tor Vergata," via del Politecnico 1, Rome 00133, Italy

1 Introduction

Soil thermal conductivity (λ) is the key property required in design and simulation of earth-contact engineering facilities that release/absorb heat to/from the surrounding ground. Examples of such applications are ground heat exchangers (heat pumps, ground heat storage), high voltage power cables, nuclear waste vaults, pipe lines, etc. In general, the ground is a porous system of an inestimable structural intricacy (soil grain and void space shapes and sizes, and unknown compaction), additionally complicated by the presence of air/water and simultaneous heat and moisture transfer phenomena. Because of these reasons and experiment-related obstacles such as unknown thermal contact resistance, sample non-homogeneity, soil moisture re-distribution, and limitations of measuring tools, the soil λ is very difficult to measure and predict accurately.

As a result, availability of reliable λ data is very limited. The existing λ data have been measured by steady-state and transient techniques, both having their own advantages and drawbacks. The guarded hot-plate (GHP) technique is a standard steady-state method with precisely specified design details and measuring procedure. However, it is bulky and requires higher ΔT across the soil sample and a very long time to reach thermal equilibrium. This technique has been successfully applied only to dry soils and under laboratory conditions. Transient techniques are portable, offer short time measurements, and are applicable to any soil water content condition. For these reasons, a thermal conductivity probe (TCP) is nowadays the most commonly used measuring tool.

The probe operation is based on line-heat source theory derived from a general model of transient heat conduction in a homogeneous isotropic material of uniform T. In reality, each probe possesses distinctive thermal characteristics that influence, in a unique way, the measurement procedure. Hence, the probe technique is still not a standardized method of λ measurement. Therefore, any researcher using the TCP bears a responsibility for providing proof (a validation test) that the probes used produce accurate and precise λ data. So far, 1 % *agar-gelled water* is the most frequently used reference material for probe validation. Its composition, contact resistance with the probe, and λ value are, however, very different from a large majority of unsaturated granular materials. Consequently, there is a growing demand for reference granular materials, with λ and texture similar to common mineral soils, which could be used for TCP validation purposes.

Reference soils should have repeatable physical characteristics (grain size distribution and mineral composition), well established λ data over a wide range of compaction ($\theta_s = \rho_b/\rho_s$; ρ_b = bulk density; ρ_s = density of solids) and T at dryness and saturation, and similar structure to soils undergoing testing. The available λ_{dry} records for these soils, however, are generally limited to single T and/or porosity ($n = 1 - \theta_s$). Therefore, the primary objective of this article is to develop a comprehensive λ_{dry} database for commonly used standard sands. The measured λ data are very often limited to just a few experimental points and do not cover a full range of wetness, which is usually required in the mathematical simulation of heat and mass transfer in soils. For this reason, predictive λ models are in great demand; for example, a simple normalized λ equation requires an input of reliable λ_{dry} and λ_{sat} data. Numerous modeling

attempts were made in the past to predict λ_{dry} and λ_{sat} from basic and easy-to-obtain soil characteristics. While λ_{sat} can be successfully predicted by a weighted geometric mean model, estimations of λ_{dry} are so far fruitless. Hence, the secondary objective of this article is to model the measured λ_{dry} data as a function of λ of air and solids (λ_a; λ_s), n, and T. In addition, λ_{dry} of high quartz content sands displays a small λ increase with increasing T, which contradicts the decreasing trend of the quartz thermal conductivity (λ_q) versus T. Therefore, the third objective is to elucidate the behavior of dry quartz sands with increasing T.

2 Review of Literature

A review of published literature [1,2] reveals three standard soils that meet most requirements for reference granular materials, namely, *Ottawa Sand 20/30* (*C-190*), *Ottawa Sand graded* (*C-109*), and *Toyoura sand*. The first two sands are well known in America, while *Toyoura* is the standard sand in Japan. The thermal conductivity λ of coarse Ottawa sand (*C-190*) was measured in the past using a GHP apparatus [3–7] and the probe technique [8–14]. Recently, Nikolaev et al. [7] carried out λ measurements at $n = 0.33$ and T from 2 °C to 92 °C at 10 °C increments. Bligh and Smith [9] measured λ at $n = 0.32$ and T from 23 °C to 25 °C while Yun and Santamariana [14] measured λ at $T = 20$ °C and $n = 0.34$ to 0.412. The thermal conductivity λ of *Toyoura sand* was measured by Momose and Kasubuchi [2] at $n = 0.4$ and T from 10 °C to 75 °C. So, in general, there is a lack of a comprehensive λ database for *Ottawa* and *Toyoura sands*. The existing λ data by [7] show a tiny λ increase with T in spite of a strong decreasing trend of λ_q. Farouki [1] suggested that quartz grain interfacial effects, prompted by a T increase, were responsible for the improved heat transfer. In turn Sakaguchi et al. [15] observed an opposite phenomenon in low moisture *Toyoura sand*, i.e., its λ was decreasing with T. It was concluded that the decrease in λ with an increase in T was mainly due to decreased water thermal bridges. No further research, however, has yet been carried out on dry pure quartz sands to elucidate this apparent anomaly.

3 Physical Characteristics of Standard Sands

Ottawa sands are composed almost entirely of natural silica (SiO_2), which are commonly used as standard sands for concrete testing (ASTM-C778-80), and are available from Ottawa Silica Co., Ottawa, IL, USA (http://www.u-s-silica.com/prodindex.htm). The most frequently tested sands are 20/30 (*C-190*) and graded sand (*C-109*). In general, *Ottawa sands* are made of sub-rounded quartz grains of a tri-axial shape described by three significant in-length axes [16] while de Vries [17] assumed that sand particles were made of rotated ellipsoids whose axis length ratio was 1:1:6. The sand *C-190* is poorly graded with all grains (mean $d_{50} = 0.72$ mm) passing through a sieve size of 0.85 mm (No. 20) and 97 % retained on a sieve size of 0.60 mm (No. 30). *C-109* is a pure quartz sand consisting of sub-rounded grains between 0.425 mm and 0.150 mm (mean $d_{50} = 0.33$ mm); more than 50 % of the grains pass through a No. 40 sieve. According to Ayoubian and Robertson [18], n of these sands vary from 0.45

Table 1 *Standard sands*: typical physical characteristics

Soil name	Quartz (%)	Feldspar (%)	Magnetite (%)	Grain type	Grain size (mm)	d_{50} (mm)	ρ_s ($kg \cdot m^{-3}$)
C-109	99.7	0	0	Sub-rounded	0.15–0.60	0.33	2650
C-190	99.8	0	0	Sub-rounded	0.60–0.85	0.72	2650
Toyoura	75.0	22	3	Sub-angular	0.1–0.2	0.167	2630

(loose compaction) to 0.33 (dense compaction). *Toyoura sand* is a well-sorted fine sand made of light brown sub-angular grains whose diameter ranges from 0.1 mm to 0.2 mm (mean $d_{50} = 0.167$ mm [16]) and is composed of 75 % quartz, 22 % feldspar, and 3 % magnetite [19]. Soil n changes from 0.49 (loose compaction) to 0.37 (dense compaction). Typical physical characteristics of three standard sands are summarized in Table 1.

The fixed content of quartz, repeatable grain size distribution, and a wide range of particle median diameter ($d_{50} \approx 0.72$ mm, 0.33 mm, and 0.167 mm) make these soils potentially suitable reference materials for validating TCP.

4 Materials and Methods

4.1 Soil Sample Preparation

Dry sands were packed into samplers made of an acrylic tube (64 mm diameter × 80 mm height). The sampler size was selected using a relationship given by de Vries and Peck [20] according to which a heat flux through the sample boundaries is small in comparison with the heat flux released by the TCP;

$$\exp\left(-\frac{r^2}{4\alpha_{\text{dry}}\tau}\right) \ll 1 \tag{1}$$

where r is the radius of a cylindrical soil sample (0.032 m), α_{dry} is the thermal diffusivity of dry soil ($2.66 \times 10^{-7}\ m^2 \cdot s^{-1}$) [9], and τ is the heating period (120 s).

For the heating period of 120 s, the value of $\exp[(-r^2/(4\alpha_{\text{dry}}\tau))] \approx 0.00033$ which is sufficient proof that soil samples were represented adequately as an infinite medium. Sand compaction was accomplished by repeatedly tapping the sampler lateral surface, and the total mass of the sand, for a specified volume, was measured. The sampler was capped with an acrylic plate having a concentric hole to accommodate the TCP handle. A TCP slide-way guide was attached to the acrylic plate to ensure vertical insertion and alignment of the probe hypodermic tube with the central axis of the soil sampler (Fig. 1).

4.2 Thermal Conductivity Probe

The TCP sheath was made of a stainless-steel hypodermic tube ($d_{\text{TCP}} = 1.06$ mm) of 55 mm effective length, ℓ_{TCP}. A T-type thermocouple was made of 0.1 mm copper/

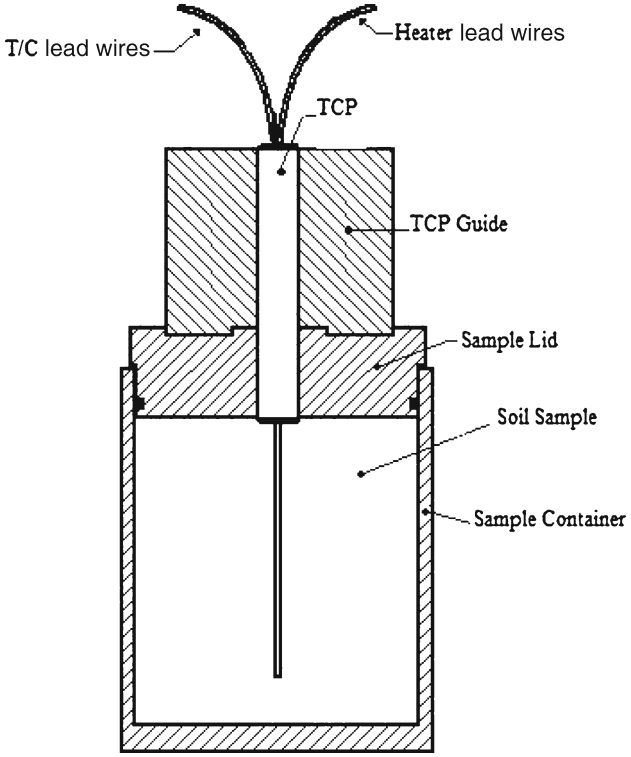

Fig. 1 Soil sampler assembly

constantan wires coated with formvar (vinyl acetal) while the probe heater was made of 0.1 mm constantan wire coated with a single polyurethane nylon (MWS Wires Industries). The heater and the thermocouple were inserted into the hypodermic tube of 0.9 mm inner diameter. The thermocouple junction was electrically insulated from the heater and the hypodermic sheath, and positioned at the point corresponding to the middle of the effective probe length ($\ell_{\mathrm{TCP}}/2$). The remaining space in the hypodermic tube was filled in with an ultra-low viscosity epoxy resin, which was subsequently cured.

The tube was fixed on a printed circuit board (PCB) containing the thermocouple and heater terminals (Fig. 2). This design allows the use of shorter heater wire and trouble-free connection of the probe extension wires of different diameters.

The wire terminals were coated with a high performance polyimide electrical insulation film (Corona) to prevent short circuits. The TCP handle was made of an acrylic tube (9 mm outer diameter and 50 mm length) and centrally placed in the PCB. The remaining space was filled with a five-minute epoxy resin. The tip of the stainless tube was blocked and smoothed. A cold junction of the thermocouple was inserted into a reference dry soil sample at the same ambient environment as the tested sand. A risk of noise due to induced voltages was minimized by twisting extension wires of the thermocouple and the TCP heater.

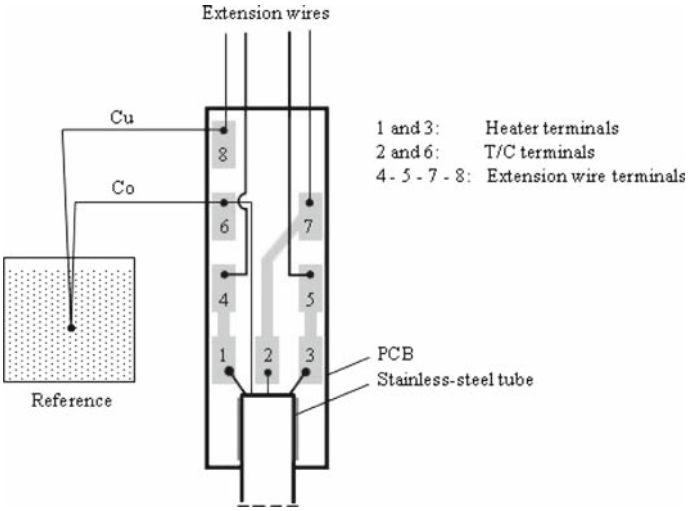

Fig. 2 Printed circuit board assembly

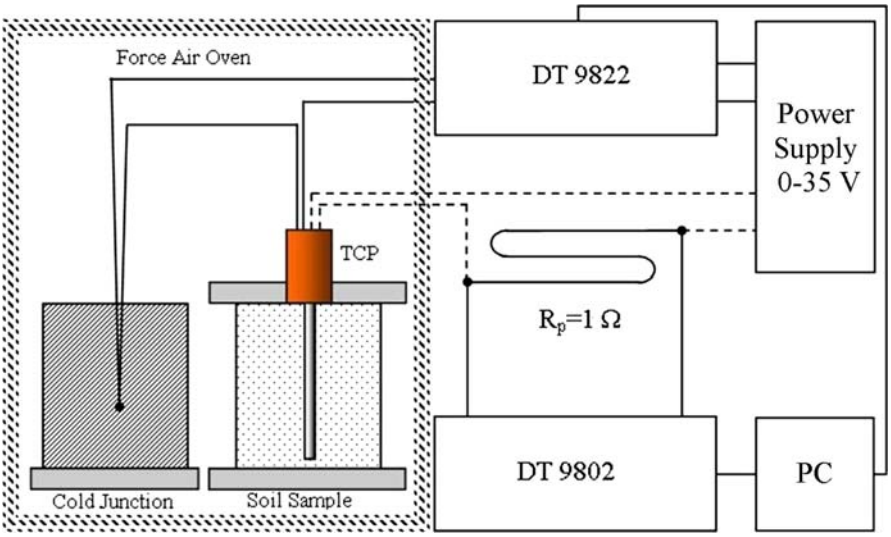

Fig. 3 Schematic diagram of experimental setup

4.3 Experimental Setup

The experimental setup of the λ measurement (Fig. 3) consists of a forced air convection oven (Memmert UE-500-AQ), TCP, two soil samplers, a constant voltage power supply, and two data acquisition systems: DT-9802 (12 bit) to record the heater current (I) and DT-9822 (24 bit) to record the thermocouple electromotive force E (in μV) and to control the heating time.

The DC power supply (HP E3611A, Hewlett-Packard Development Co.) provided a constant current (I) to the probe heater. Measuring time intervals for data records were set by the DT Foundry 5.0 software package (Data Transition, Inc.). The heater current, I, was determined through the use of a 1.0 Ω (±0.001 Ω) precision resistor (R_{pr}) while the voltage change (V_{pr}) across the R_{pr} was usually set at 70 mV (±0.3 mV). Then, I was calculated, by using the equation, $I = V_{pr}/R_{pr}$, with an uncertainty of 0.4 mA. For tests above 25 °C, a sampler with tested soil was placed in a forced air convection oven with T control of ±0.2 °C.

4.4 Line-Heat Source Technique

The line-heat source theory assumes the use of an infinitely long and infinitesimal-in-diameter line-heat source, a substantially large homogeneous and isotropic material at uniform T_0, and no contact resistance between the line-heat source and surrounding material. For these conditions, the $T - T_0$ rise at a radial distance r from the line-heat source is given by the following relation [21]:

$$T - T_0 = \frac{q}{4\pi\lambda}\left[-\mathrm{Ei}\left(-\frac{r^2}{4\alpha\tau}\right)\right] \tag{2}$$

where α is the sample thermal diffusivity, q is the linear heat source strength per unit length, τ is time, and λ is the measured thermal conductivity.

For small $r^2/4\alpha\tau$ values, compared to unity (large τ or small r), the exponential integral can be approximated by a logarithm of τ, and λ can be assessed from the relation,

$$\Delta T \approx \frac{q}{4\pi\lambda}\ln(\tau) + c \quad \text{for} \quad \tau_1 < \tau < \tau_2 \tag{3}$$

where $\Delta T = T - T_0$, τ_1 is the end of a probe transitory heating period, τ_2 is the time at which the heating process is completed, and c is a constant.

The actual probes, however, produce ΔT deviations, from that given by Eq. 3, caused mainly by the probe finite dimensions (length and diameter), mass, heat capacity, different thermal properties than the tested material samples, and thermal contact resistance at the probe surface [22]. These problems can be practically eliminated by using a long enough probe of small diameter and a suitable heating time [23]. When $\ell_{TCP}/d_{TCP} > 50$, the TCP acts practically as a perfect line heat source [24]. The time period of probe heating was set to 120 s which is well below the approximate time when the soil T shows any sign of change at the sampler lateral border just confirming that the soil sample simulates an infinite medium. To minimize the thermal contact resistance effect, a much larger probe diameter (1.06 mm) than the d_{50} of the tested sands was used. Three matching sand samples were tested simultaneously over a wide range of T and n (4 to 5 different soil compactions). The oven T was set at (25, 40, 50, 60, and 70) °C, and the thermal equilibrium of the soil sample and TCP with the oven environment was usually reached after approximately 4 h. For each sample (fixed n and T), λ measurements were repeated at least three times and then the λ values were averaged. After the λ measurement at 70 °C was completed, the soil sample was

Table 2 *C-190*: summary of TCP validation versus GHP

C-190	n	T (°C)	λ_{GHP} ($W \cdot m^{-1} \cdot K^{-1}$)	λ_{TCP} @ 25 °C ($W \cdot m^{-1} \cdot K^{-1}$)	Δ(%)
Kersten [3]	0.41	21.1	0.255	0.249	2.4
Woodside and Cliffe [4]	0.40	23.9	0.264	0.249	5.7
Nikolaev et al. [7]	0.33	22	0.322	0.324	−0.6
				% Error	**2.5**

cooled to 25 °C and the λ test was repeated again and all λ data at 25 °C were evaluated. In case of any noticeable data variance, the entire set of experiments was repeated. Next, the E voltage was converted to ΔT and the slope m was evaluated. In general, collected data (ΔT versus τ) at the beginning of the heating period do not perfectly satisfy Eq. 2. Therefore, to reduce the influence of the probe thermal inertia and the contact resistance (at the probe–soil interface), and to consider a larger volume of soil around the probe for λ evaluation [23], the data from the first 20 s (τ_1) of heating was ignored. Then, λ of a tested sample was assessed from the following relation:

$$\lambda \approx \frac{q}{4\pi m} \tag{4}$$

where m is the slope of a linear portion of ΔT versus $\ln(\Delta\tau)$, $\Delta T = T_2 - T_1$, $\Delta\tau = \tau_2 - \tau_1$, $q = I^2 R_h / \ell_{TCP}$, I is the heater current, R_h is the electrical resistance of the heater, ℓ_{TCP} is the effective length of the TCP, and λ is the thermal conductivity of the tested material.

During the TCP heating period, a total of 1500 data pairs of τ and E were recorded at a fixed I supplied to the TCP. The quality of the slope linear relation, ΔT versus $\ln(\Delta\tau)$, was evaluated by using a correlation coefficient $r^2 > 0.99$, but a residual analysis and Fisher test could also be applied. In order to maintain a small increase in T of the probe ($T < 4$ °C), a current of 70 mA was supplied to the heater for testing the probe with 1 % agar gel and dry sands. Thus, the TCP source strength was about $1.1\ W \cdot m^{-1}$.

5 Probe Validation Tests

Theoretical evaluation of the probe measuring accuracy is highly unrealistic due to several unique inadequacies introduced during the probe manufacturing process. Therefore, each newly built TCP was at first validated against reference materials for which λ data had been obtained by standard methods of measurement. So, the probe validation was conducted with the standard reference medium of 1 % agar-gelled distilled water at T of (25, 40, 50, 60, and 70) °C. The experimental data (λ_{TCP}) obtained was compared against λ of water (λ_{ref}) published by Sengers and Watson [25]. This procedure was repeated at least three times at each T, and then the average value was taken. The ratios $\lambda_{TCP}/\lambda_{ref}$ were not T dependent, and a relative error of the validated probes ranged from 0.3 % to 2.7 %. Then, the probe validation was checked against λ data of *C-190* and *C-109* measured by GHP apparatus (Tables 2, 3).

Table 3 *C-109*: summary of TCP validation versus GHP

C-109	*n*	*T* (°C)	λ_{GHP} ($W \cdot m^{-1} \cdot K^{-1}$)	λ_{TCP} @ 25 °C ($W \cdot m^{-1} \cdot K^{-1}$)	Δ (%)
Kersten [3]	0.41	21.1	0.254	0.250	1.6
				% Error	**1.6**

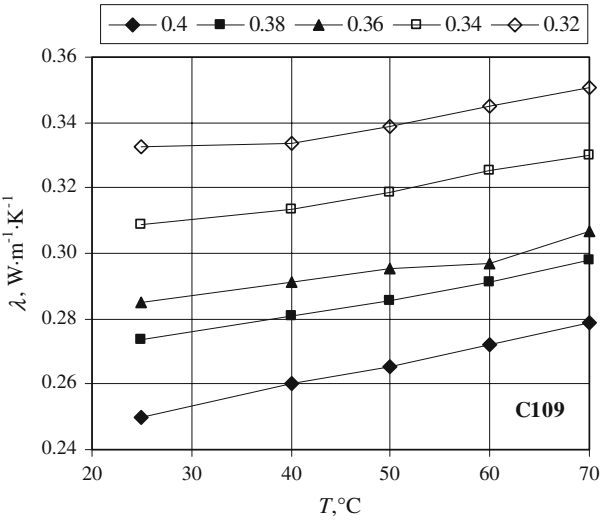

Fig. 4 $C - 109$: λ_{dry} versus T and n

According to Manohar et al. [26], the probe method provides reliable and repeatable measurements, for homogeneous granular materials, within ±3.5 % error. The maximum relative error between λ_{TCP} and λ_{GHP} was, on average, about 2.0 %, thus providing sufficient proof that the TCPs used were reasonably accurate.

6 Results and Discussion

Experimental λ data for dry *C-109, C-190*, and *Toyoura sand* are summarized in the Appendix. The λ_{dry} dependence versus n, for varying T, for dry *C-109, C-190*, and *Toyoura sand* is displayed in Figs. 4, 5, and 6, respectively. It is evident that λ_{dry} increases with T, and the rate of increase gradually decreases as n (content of air) decreases. This tendency suggests that air surrounding the quartz grains act as a very effective thermal resistor which minimizes the decreasing λ_q trend with T. So, higher air content means stronger λ_{dry} increase with T. A careful analysis of the obtained data reveals that for $n = 0.4$ and a full range of T, *Toyoura sand*, in spite of a lower content of quartz than *C-109*, has very similar λ values to *C-109* and greater λ values than *C-190*. This outcome can be explained by the diverse grain size distribution of tested sands. The sand *C-190* consists of relatively large sub-rounded particles ranging

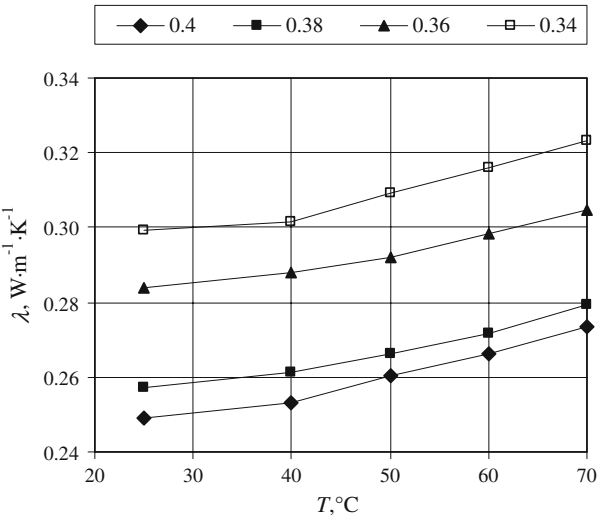

Fig. 5 *C − 190*: λ_{dry} versus T and n

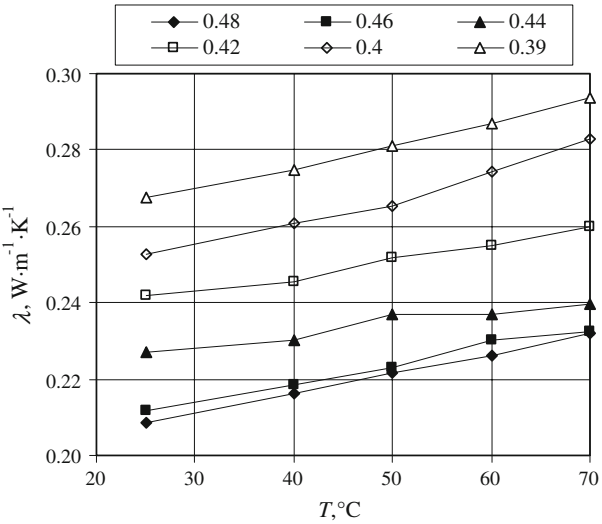

Fig. 6 *Toyoura sand*: λ_{dry} versus T and n

from 0.65 mm to 0.85 mm (97 %); *C-109* is composed of three large grain fractions: 0.425 mm to 0.6 mm (28 %); 0.3 mm to 0.425 mm (45 %); and 0.15 mm to 0.3 mm (23 %); while *Toyoura sand* is composed largely of fine particles ranging from 0.1 mm to 0.2 mm. Besides, $n = 0.4$ means loose compaction for *C-109* and *C-190*, while for *Toyoura sand*, it is a dense compaction featuring better inter-particle contacts and thus enhanced interfacial heat conduction of the solid framework. Consequently, a denser compaction of *Toyoura sand*, with respect to *C-109*, leads to smaller air voids, increased particle-to-particle contact areas, and thus increased λ_{dry}. In turn, *C-109*

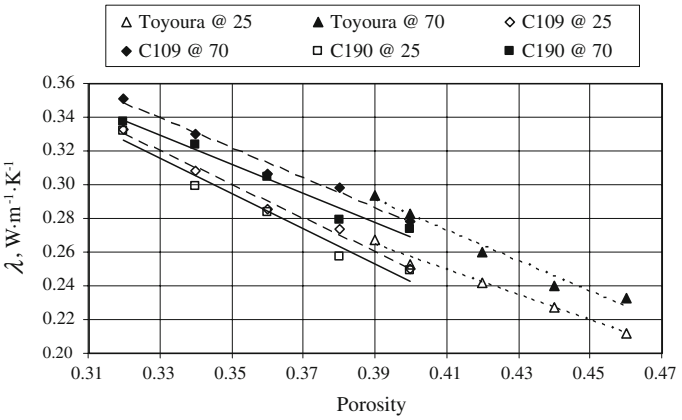

Fig. 7 Thermal conductivity of quartz sands versus n and T (25 °C and 70 °C)

is a well graded sand, as opposed to *C-190*, whose smallest grains act as a binder between larger grains, enhancing particle-to-particle contacts and consequently leading to slightly higher λ_{dry} than for *C-190*.

The trends of λ_{dry} versus n and T, for *C-109, C-190*, and *Toyoura sand*, are shown in Fig. 7.

In general, λ_{dry} decreases linearly with increasing n and gets slightly larger with an increase in T. An increase in n means getting more loose grain compaction, i.e., reduced inter-particle contacts and consequently lower λ_{dry}. For both *Ottawa sands* the decreasing trends of λ_{dry} are very similar at both 25 °C and 70 °C. *Toyoura sand* has a similar λ_{dry} dependence on n and T.

7 Uncertainty Analysis

Type A and Type B uncertainties were evaluated based on ISO recommendations [27]. The Type A uncertainty refers to uncertainty prediction of the slope m (ΔT versus $\ln(\Delta\tau)$) by a least-squares procedure [28] and statistics of repeated measurements on the same and other materials. Based on repeated λ measurements of 1 % *agar-gelled* distilled water, *C-109, C-190*, and *Toyoura* sands, from 25 °C to 70 °C, the Type A uncertainty was less than 1.4 %. The Type B includes all other uncertainty sources that are not evaluated by statistical methods, i.e., propagation of uncertainty in evaluating the λ value, effect of environmental conditions, and knowledge of the measuring procedures published in scientific literature. Therefore, the uncertainty propagation of measurements (T, V, R_h, ℓ_{TCP}) was assessed. Using the expression for the probe heating flux $\left(q = V^2/(R_h \ell_{TCP})\right)$, and taking into account its dependence on V, the uncertainty propagation is expressed as follows:

$$\left(\frac{\Delta\lambda}{\lambda}\right)^2 = \left(2\frac{\Delta I}{I}\right)^2 + \left(\frac{\Delta R_h}{R_h}\right)^2 + \left(\frac{\Delta \ell_{TCP}}{\ell_{TCP}}\right)^2 \tag{5}$$

Table 4 Summary of relative systematic errors

Variable	Typical value	$\Delta x/x$
I	0.07 A	0.57 %
R_h	12.5 Ω	0.10 %
ℓ_{TCP}	55 mm	0.20 %

Typical values and respective uncertainties are summarized in Table 4.

Using the above data (Table 4) and Eq. 5, the relative Type B uncertainty was about 1.2 %. Combining Type A and Type B uncertainties in quadrature gives a total uncertainty of about 1.8 %.

8 Modeling Approaches

Dry quartz sands can be modeled as two-phase systems with continuously changing fractions (θ) of dry solids and air; solids are composed mainly of quartz while air is acting as an effective thermal resistor. The λ data of these sands is relatively straightforward to model as the mineralogical composition, grain size, and λ data of basic components (quartz and air) are very well established. The quartz structure is non-isotropic, and λ varies with the direction of heat flow and also with T. The thermal conductivity λ parallel to the quartz optic axis ($\lambda_{q-\parallel} = 11.3\,W \cdot m^{-1} \cdot K^{-1}$) is higher than that in the perpendicular direction ($\lambda_{q-\perp} = 6.5\,W \cdot m^{-1} \cdot K^{-1}$). Therefore, the total λ of randomly oriented quartz crystals is usually evaluated as a weighted geometric mean [1];

$$\lambda_q = \lambda_{q-\parallel}^{1/3} \lambda_{q-\perp}^{2/3} \tag{6}$$

The T dependence of the total λ_q, based on quartz data by Clauser and Huenges [29] and Eq. 6, can be obtained by the following equation ($0 < T < 100\,°C$):

$$\lambda_q = 8.128 - 0.021T \qquad (r^2 = 0.9927) \tag{7}$$

At $T = 20\,°C$, λ_q is $7.7\,W \cdot m^{-1} \cdot K^{-1}$; and this value is similar to that used by Johansen [30] and Horai [31].

The T dependence of the thermal conductivity of dry air (λ_a) can be described by the following equation ($0 < T < 100\,°C$):

$$\lambda_a = 0.0243 + 0.00007T \qquad (r^2 = 0.9999) \tag{8}$$

The rate of the increase of λ_a with T is much smaller than the decreasing trend of λ_q. λ_{dry} is influenced mainly by n, and to a lesser degree by λ of sand components (i.e., quartz and air), T, and soil texture. The rate of σ (λ_q/λ_a) is T dependent and has a very high value ($\lambda_q/\lambda_a \approx 225$ to 290); therefore, none of the simple classical models (series, parallel, and geometric mean) offers acceptable λ_{dry} predictions. From a review of the relevant literature on two-phase models [1,9,14,32,33], only the model by de Vries [33] and the series-parallel model by Woodside and Messmer [34] have

Table 5 *RRMSE* (%) summary

Soil name	De Vries (Eq. 10)	Woodside–Messmer (Eq. 12)
C-109	2.78	1.80
C-190	2.23	2.81
Toyoura sand	2.60	2.37

been considered. The performance of these models was assessed by using the root relative mean square error (*RRMSE*),

$$RRMSE = \sqrt{\frac{1}{N}\sum_{1}^{N}\left[\frac{\lambda_{\exp}-\lambda_{\mathrm{cal}}}{\lambda_{\exp}}\right]^2} \tag{9}$$

8.1 de Vries Model (deV)

de Vries [17] modified the model by Eucken [35] and introduced a number of subjective assumptions such as all soil particles have a shape of rotated ellipsoids, with a length of the minor axis of $g_1 = g_2 = g_{1-2} = 0.125$ and the major axis ($g_3 = 1-2\cdot g_{1-2} = 0.75$) six-times longer, and being randomly suspended in the continuous medium and not contacting each other.

$$\lambda_{\mathrm{dry}} = \lambda_{\mathrm{a}}\frac{n+(1-n)k_{\mathrm{s-f}}\sigma}{n+(1-n)k_{\mathrm{s-f}}} \tag{10}$$

$$k_{\mathrm{s-f}} = \frac{1}{3}\left\{\frac{2}{1+[\sigma-1]g_{1-2}} + \frac{1}{1+[\sigma-1](1-2g_{1-2})}\right\} \tag{11}$$

where $k_{\mathrm{s-f}}$ is the weighting shape factor. In reality, the assumed $k_{\mathrm{s-f}}$ has very little to do with the actual shape of soil grains and, therefore, it is usually treated as a fitting parameter.

de Vries applied $g_{1-2} = 0.125$ and $k_{\mathrm{s-f}} \approx 0.02$ to dry quartz sand, 89 % of quartz and 11 % of feldspar at 20 °C, and reported that estimated λ_{dry} values had to be multiplied by a correction factor of 1.25 to make the results consistent with measured data. Johansen [30] used a slightly different particle ellipsoidal shape value ($g_{1-2} = 0.1$) and a fixed value of $\lambda_{\mathrm{s}} = 3\,\mathrm{W}\cdot\mathrm{m}^{-1}\cdot\mathrm{K}^{-1}$ to model experimental data by Smith and Byers [36], Smith [37], and 11 personally tested soils, and obtained $k_{\mathrm{s-f}}$ of about 0.0531. When these particle shape factors were applied to pure quartz sands ($\lambda_{\mathrm{s}} = \lambda_{\mathrm{q}} = 7.57\,\mathrm{W}\cdot\mathrm{m}^{-1}\cdot\mathrm{K}^{-1}$ at 25 °C), largely over-estimated λ_{dry} values were obtained. Therefore, for modeling λ_{dry} of quartz sands the following input data were used: λ_{q} from Eq. 7 and λ_{a} from Eq. 8, particle shape values (g_{1-2}) for *C-109* (0.12); *C-190* (0.125); and for *Toyoura* sand (0.11), and the model produced good fits to all experimental data without the need for a correction factor. In addition, $k_{\mathrm{s-f}}$ depends linearly on T and ellipsoid shape values g_{1-2} (Fig. 8).

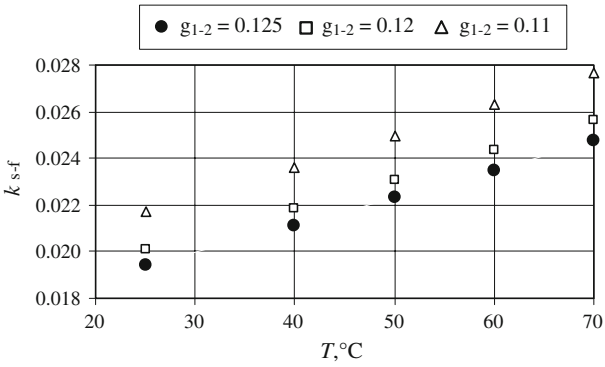

Fig. 8 Weighting shape factor k_{s-f} versus T and g_{1-2}

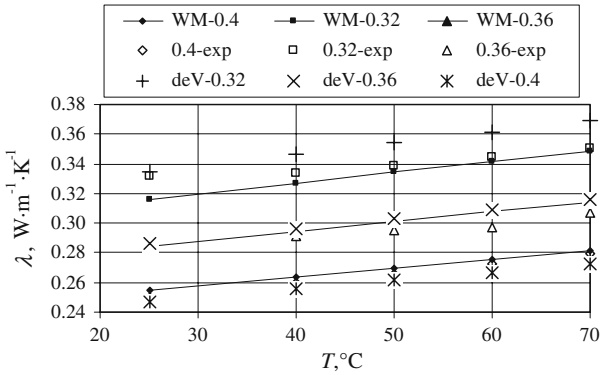

Fig. 9 *C-109*: experimental λ_{dry} data versus model predictions at three different porosities

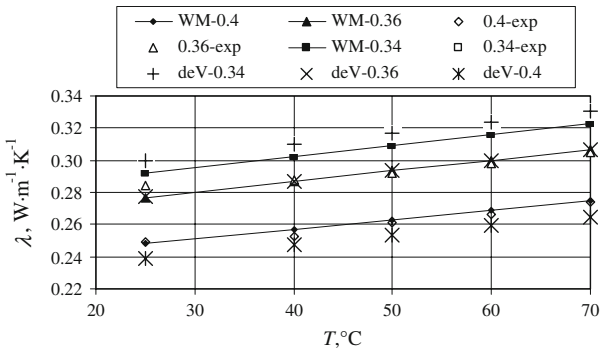

Fig. 10 *C-190*: experimental λ_{dry} data versus model predictions at three different porosities

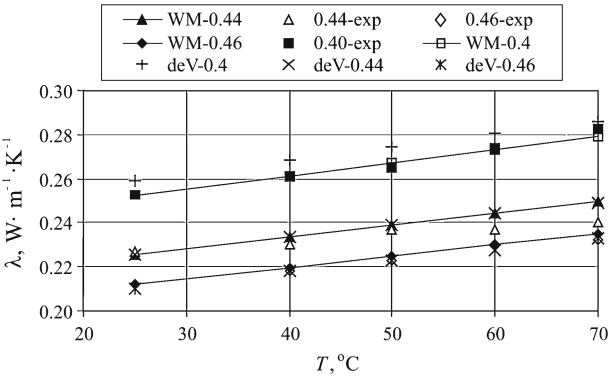

Fig. 11 *Toyoura sand*: experimental λ_{dry} data versus model predictions at three different porosities

The model by de Vries, with modified λ_q, predicts the experimental data exceptionally well with an average *RRMSE* of 2.54 % (Figs. 9–11).

8.2 Series-Parallel Model (WM)

This relation, proposed by Woodside and Messmer [34], considers two paths along which heat is conducted through a system of soil grains, namely, a continuous path through the major portion of soil air and a series-parallel path through the solid grains bridged with a small portion of soil air. The model can be expressed in the following form:

$$\lambda_{dry} = \lambda_a (n - n_{WM}) + \frac{(1 - n + n_{WM})^2}{\frac{1-n}{\lambda_s} + \frac{n_{WM}}{\lambda_a}} \tag{12}$$

where n_{WM} is the fluid fraction in a series path of heat flow.

In general, n_{WM} depends on the soil grain size, n, and also on λ_s and λ_a that are T dependent; generally, loose compaction indicates higher n_{WM} values. At both extreme ends of n range (0 and 1), n_{WM} is very close to zero, while for n corresponding to tested sands (0.32 to 0.46), n_{WM} was on average around 0.0415, 0.0428, and 0.0412 for *C-109, C-190*, and *Toyoura sand*, respectively. λ for solids (λ_s) was obtained from the following relation:

$$\lambda_s = \lambda_q^{\theta_q} \lambda_{o-min}^{1-\theta_q} \tag{13}$$

where θ_q is the volumetric content of quartz and λ_{o-min} is the thermal conductivity of minerals other than quartz (usually about $2\,W \cdot m^{-1} \cdot K^{-1}$).

The series-parallel model (Eq. 12) predicts the experimental data with an average *RRMSE* of 2.33 % (Figs. 9–11).

In summary, the models by de Vries (Eq. 10, 11) and by Woodside–Messmer (Eq. 12) predict the experimental λ data with *RRMSE* less than 2.81 % (Table 5).

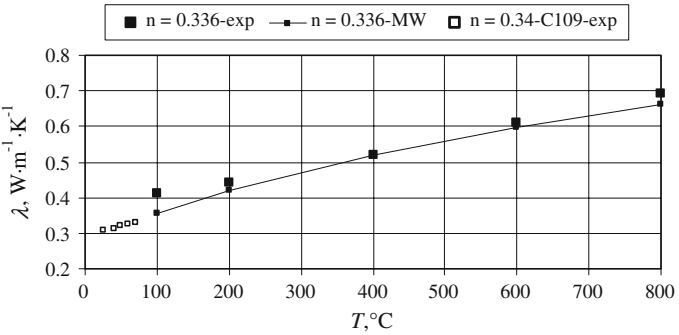

Fig. 12 *C-109*: experimental and predicted λ_{dry} at elevated T ($n = 0.34$)

The series-parallel model (Eq. 12) was also applied to *C-109* at elevated T from 100 °C to 800 °C [38]. Figure 12 shows comparisons of experimental data versus predictions by the series-parallel model (Eq. 12) for a full range of T (25 °C to 800 °C).

For close compaction ($n = 0.34$), λ predictions by a series-parallel model show good agreement with experimental [38] data which provide additional proof on the insulation effect of air in the dry pure quartz sands.

8.3 Thermal Conductance Model

Careful examination of λ predictive models reveal that, in general, λ_{dry} can be modeled as a product of λ_s and a normalized thermal conductance factor κ ($0 \leq \kappa \leq 1$);

$$\lambda_{dry} = \lambda_s \kappa \tag{14}$$

Diminishing values of κ mean a stronger insulation effect of air and consequently lower λ_{dry}.

In general, κ is dependent on σ and n and can be evaluated from the following relations:

$$\kappa_{exp} = \frac{\lambda_{dry-exp}}{\lambda_s} \tag{15}$$

$$\kappa_{deV} = \frac{n\frac{1}{\sigma} + (1-n)\,k_{s-f}}{n + (1-n)\,k_{s-f}} \tag{16}$$

$$\kappa_{WM} = \frac{(n - n_{WM})}{\sigma} + \frac{(1 - n + n_{WM})^2}{1\text{-}n + n_{WM}\sigma} \tag{17}$$

Figure 13 displays κ versus n ranging from 0 to 1 (solids to air) for six sandstones studied by Woodside and Messmer [39]. The experimental λ_{dry} data, at 30 °C, cover a wide range of n (0.0263, 0.105, 0.155, 0.22, 0.29, and 0.59) and represent sandstones having a high content of quartz varying from 85 % to 98 %. Therefore, it is very convenient to use these data for modeling κ over the full range of n. For the de Vries model

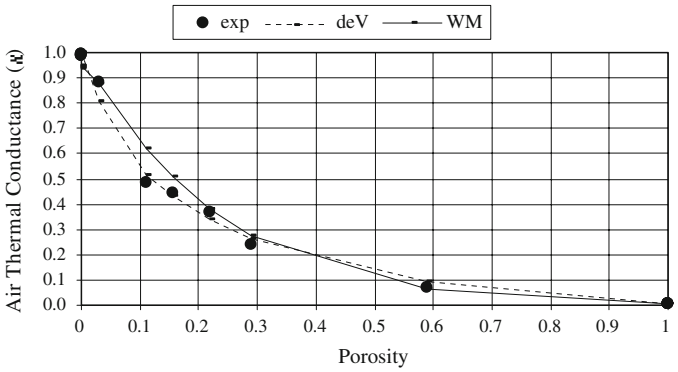

Fig. 13 *Quartz sandstones*: thermal conductance factor (κ) versus n

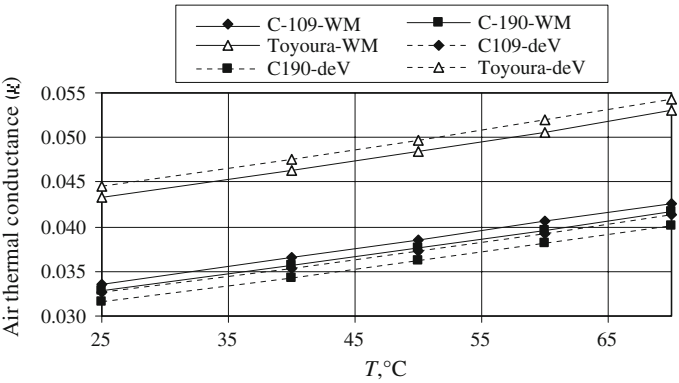

Fig. 14 *Quartz sands*: thermal conductance factor (κ) versus T ($n = 0.4$)

(deV), the particle ellipsoidal shape factor (g_{1-2}) was assumed to be 0.015, while for the Woodside–Messmer model (WM), n_{WM} was calculated from an empirical relation applied to a full range of n;

$$n_{\mathrm{WM}} = 0.000241 - 0.04376n^2 \ln(n) \qquad (r^2 = 0.94) \tag{18}$$

κ_{deV} (Eq. 16) follows closely the κ_{exp} trend, and it is easier to model as k_{s} does not depend on n, in contrary to n_{WM}. κ_{WM} overpredicts κ_{exp} in a low n range as each sandstone has a distinctive κ_{WM} value due to its diverse texture, different n, and λ_{s}, while κ_{deV} appears to follow well a general κ_{exp} trend over the full n range. Due to large values of $\lambda_{\mathrm{s}}/\lambda_{\mathrm{a}}(\sigma > 242)$, the κ factor is rapidly decreasing with n, and for $n = 0.59$, it approaches $\kappa_{\mathrm{exp}} \approx 0.07$. The results displayed in Fig. 13 confirm that the proposed air thermal conductance models (Eqs. 16, 17) can also be applied to pure and semi-clean quartz sands provided that new fitting parameters (g_{1-2} and n_{WM}) are applied. Due to a lack of experimental λ_{dry} data at very low n, the κ analysis of the quartz sands under investigation was limited to $n = 0.4$ (Fig. 14).

For the same type of sand, both κ_{WM} and κ_{deV} have similar values and a similar slope against T. A small disparity in κ values is due to differences in soil texture (n_{WM}), λ_s/λ_a, and grain shape factor (g_{1-2}).

9 Conclusions and Recommendations

A comprehensive thermal conductivity database of three dry standard sands (Ottawa *C-109*, Ottawa *C-190*, and *Toyoura*) was developed using a transient line-heat source technique. The database contains λ data representing a variety of soil compactions and temperature ranging from 25 °C to 70 °C. The tested standard sands, due to their repeatable physical characteristics, can be used as reference materials for the validation of thermal probes applied to similar dry granular materials. The measured data show an increasing λ_{dry} trend with increasing T in spite of decreasing λ_q with T. The highest slope of λ_{dry} versus T was observed for loose soil compactions (large content of air). Its value gradually disappeared with the increasing compaction of sand (decreasing content of air). This phenomenon confirms the dominant influence of air on λ_{dry}; the air surrounding the soil particles act as a very effective thermal resistor that neutralizes the decreasing trend of λ_q with increasing T. The experimental λ_{dry} data were exceptionally well predicted by de Vries and by Woodside–Messmer models, with *RRMSE* ranging from 1.80 % to 2.81 %, and can also be modeled by the thermal conductance model, a product of λ_s and κ. The value of κ is strongly influenced by the soil n and to a smaller extent by the T-dependent λ_s and λ_a and soil grain size distribution. The developed λ database is limited to the sand dry state; therefore, it would be beneficial to develop a comprehensive λ database for the same standard sands saturated with water.

Acknowledgments This work was supported by the Natural Sciences and Engineering Research Council of Canada and Saint Mary's University. The authors would like to express profound gratitude to Dr. Bernhard Wagner (Bavarian Geological Survey, Germany) and Prof. Tatsuaki Kasubuchi (Yamagata University, Japan) for their constructive comments during final preparation of the manuscript. Appreciation is extended to Mr. Jeff Levy for designing and manufacturing the probe printed circuit board and Mr. Samir Metlej for manufacturing and testing the thermal conductivity probes.

Appendix

Table A-1 Dry *C-109*: thermal conductivity ($W \cdot m^{-1} \cdot K^{-1}$) versus T and n

C-109					
T(°C)	n				
	0.40	**0.38**	**0.36**	**0.34**	**0.32**
25	0.250	0.274	0.285	0.309	0.332
40	0.260	0.281	0.291	0.313	0.334
50	0.266	0.285	0.295	0.319	0.339
60	0.272	0.291	0.297	0.325	0.345
70	0.279	0.298	0.307	0.330	0.350

Table A-2 Dry *C-190*: thermal conductivity ($W \cdot m^{-1} \cdot K^{-1}$) versus T and n

C-190				
T(°C)	n			
	0.40	**0.38**	**0.36**	**0.34**
25	0.249	0.257	0.284	0.299
40	0.253	0.261	0.288	0.302
50	0.261	0.266	0.292	0.309
60	0.266	0.272	0.298	0.316
70	0.274	0.279	0.305	0.323

Table A-3 Dry *Toyoura sand*: thermal conductivity ($W \cdot m^{-1} \cdot K^{-1}$) versus T and n

Toyoura sand					
T(°C)	n				
	0.46	**0.44**	**0.42**	**0.40**	**0.39**
25	0.212	0.227	0.242	0.253	0.267
40	0.218	0.230	0.246	0.261	0.275
50	0.223	0.237	0.252	0.265	0.281
60	0.230	0.237	0.255	0.274	0.287
70	0.232	0.240	0.260	0.283	0.294

References

1. O.T. Farouki, in *Thermal Properties of Soils. Series on Rock and Soil Mechanics*, vol. 11 (Trans Tech Publication, Clausthal-Zellerteld, 1986)
2. T. Momose, T. Kasubuchi, Eur. J. Soil Sci. **53**, 599 (2002)
3. M.S. Kersten, in *Thermal Properties of Soils* (University of Minnesota, Minneapolis, 1949)
4. W. Woodside, J.B. Cliffe, Soil Sci. **87**, 75 (1959)
5. W.A. Slusarchuk, P.H. Fougler, in *Technical Paper No. 388*, Division of Building Research, National Research Council of Canada (1973)
6. F.D. Haynes, D.L. Carbee, D.J. VanPelt, in *Special Report 80-83*, Cold Regions Research and Engineering Lab, Hanover, NH (1980), p. 33
7. I. Nikolaev, D.O. Reid, W.H. Leong, M.A. Rosen, in *Proceedings of the 21st Canadian Congress of Applied Mechanics* (2007), pp. 378–379
8. M.A. Sophocleous, Water Resources Res. **15**, 1195 (1979)
9. T.P. Bligh, E.A. Smith, in *EEBS Report No. 26*, MIT Joint Program, Energy Efficient Buildings and Systems (1983), pp. 1–275
10. A.F. Moench, D.D. Evans, Soil Sci. Soc. Am. Proc. **34**, 377 (1977)
11. K.W. Jackson. PhD Thesis (Georgia Institute of Technology, Atlanta, GA, 1980)
12. S.I. Park, J.G. Hartley, J. Appl. Phys. **86**, 5263 (1999)
13. S. Corasaniti, G. Pasquali, P. Coppa, in *Proceedings of IX A.I.P.T Meeting*, Torino (2004), pp. 45–56
14. T.S. Yun, J.C. Santamarina, Granular Matter **10**, 197 (2008)
15. I. Sakaguchi, T. Momose, T. Kasubuchi, Eur. J. Soil Sci. **58**, 92 (2007)

16. T. Matsushima, K. Konagai, in *Geomechanics Proceedings* (2001), pp. 361–366.
17. D.A. de Vries, in *Physics of the Plant Environment*, ed. by W.R. Wijik (North Holland Publishers, Amsterdam, 1963), pp. 210–235
18. A. Ayoubian, P.K. Robertson, Can. Geotech. J. **35**, 351 (1998)
19. M. Oda, I. Koishikawa, T. Higuchi, Soils Found. **18**, 25 (1978)
20. D.A. de Vries, A.I. Peck, Aust. J. Phys. **11**, 255–271 (1958)
21. H.S Carslaw, J.C. Jaeger, *Conduction of Heat in Solids* (Clarendon Press, Oxford, 1959)
22. E.G. Murakami, V.E. Sweat, S.K. Sastry, E. Kolbe, J. Food Eng. **30**, 209 (1996)
23. S. Shiozawa, G.S. Campbell, Remote Sens. Rev. **5**, 301 (1990)
24. A.E. Wechsler, in *Compendium of Thermophysical Property Measurement Methods*, *Recommended Measuring Techniques and Practices*, vol. 2, ed. by K.D. Maglić, A. Cezairliyan, V.E. Peletsky (Plenum Press, London, 1992)
25. J.V. Sengers, J.T.R. Watson, J. Phys. Chem. Ref. Data **15**, 1291 (1986)
26. K. Manohar, D.W. Yarbrough, J.R. Booth, J. Test. Eval. **28**, 345 (2000)
27. International Organization for Standardization, *Guide to the Expression of Uncertainty in Measurement* (ISO, Geneva, 1995)
28. S. Brandt, *Statistical and Computational Methods in Data Analysis* (North Holland Publishers, Amsterdam, 1970)
29. C. Clauser, E. Huenges, Am. Geophys. Union Ref. Shelf **3**, 105 (1995)
30. O. Johansen. PhD Thesis (University of Trondheim, Trondheim, 1975)
31. K. Horai, J. Geophys. Res. **76**, 1278 (1971).
32. R. McGaw, Highway Research Board Special Report **103**, 114 (1969)
33. D.A. De Vries, *The Thermal Conductivity of Soil* (Mededelingen van de Landbouwhogeschool, Wageningen, 1952)
34. W. Woodside, J.H. Messmer, J. Appl. Phys. **32**, 1688 (1961)
35. A. Eucken, Forsch. Geb. Ingenieurwers. **11**, 6 (1940)
36. W.O. Smith, H.G. Byers, Soil Sci. Soc. Am. Proc. **3**, 13 (1938)
37. W.O. Smith, Soil Sci. **53**, 435 (1942)
38. D.R. Flynn, T.W. Watson, in *8th Annual Conference on Thermal Conductivity* (1969), pp. 913–939
39. W. Woodside, J.H. Messmer, J. Appl. Phys. **32**, 1699 (1961)